Journal of Sound and Vibration (1998) **214**(5), 817–831
Article No. sv981552

A NEW DUAL-REACTION MASS DYNAMIC VIBRATION ABSORBER ACTUATOR FOR ACTIVE VIBRATION CONTROL

R. A. Burdisso and J. D. Heilmann

Vibration and Acoustics Laboratories, *Mechanical Engineering Department*, *Virginia Polytechnic Institute and State University*, *Blacksburg*, *Virginia* 24061-0238, *U.S.A.*

(*Received* 11 *August* 1997, *and in final form* 3 *February* 1998)

A new passive/active dynamic vibration absorber is proposed for structural vibration control. The device consists of two reaction-masses attached to the primary structure through elastic elements. The active force pair is applied between these two reaction masses. This configuration should be contrasted to the traditional single reaction-mass system where the control force pair is implemented between the reaction-mass and the primary structure. The performance of the new device is evaluated by controlling the response of a cantilever beam subjected to white noise excitation. The control approach used is the feedforward algorithm. For purposes of comparison, the results are compared to the performance of an equivalent single reaction mass device. The results show that the proposed dual-mass dynamic vibration absorber actuator achieves the same level of vibration reduction using only half the control effort required by the single reaction-mass actuator. In addition, the concept of force transmissibility function is introduced. This function is the force applied by the hybrid dynamic vibration absorber onto an infinity impedance due to a unit control force. It is demonstrated that this function is an effective means to determine the potential of these devices.

1. INTRODUCTION

Since its introduction in the early 1990's, dynamic vibration absorbers (DVA) have been successfully used to attenuate the vibration of many structures [1]. The DVA usually consists of a mass attached to the structure to be controlled through a springer–damper system. When the DVA is mounted on a larger primary structure which is excited by some disturbance, the motion of the structure around the resonant frequency of the absorber is significantly reduced. Thus, the natural frequency and damping of the absorber are selected to yield the best attenuation of the primary structure at a particular narrow frequency range. These devices have been applied to a wide range of applications in many engineering fields [2].

One of the drawbacks of traditional DVAs is that they may be tuned to only one frequency. In instances where the resonance frequencies of the primary structure and/or frequencies of the disturbance change, adaptive absorbers which can adjust their own parameters have been proposed and successfully tested. A review of adaptive DVAs can be found in the work by von Flotow *et al*. [3]. Another approach to increase the effectiveness of vibration absorbers is the implementation of an active component. This active element traditionally consists of a control force pair applied between the absorber's mass and the primary structure in parallel to the elastic element used to mount the

0022–460X/98/300817 + 15 $30.00/0

absorber. These active/passive or hybrid DVAs provide effective vibration control over a broader frequency range when compared to passive or adaptive DVAs. An excellent survey of passive, adaptive, and active DVAs was prepared by Sun *et al*. [4].

In this paper, a new hybrid DVA configuration is presented and its performance experimentally evaluated [5, 6]. A schematic of this new hybrid DVA is shown in Figure 1(a). The new DVA consists of two masses, each independently coupled to the primary structure to be controlled through elastic elements. Although not shown in the figure, the masses may also be elastically coupled to each other. In this hybrid dual-mass DVA (DM-DVA) the active force is applied between the two masses. This configuration should be contrasted to the traditional hybrid single mass DVA (SM-DVA) configuration shown in Figure 1(b). The traditional SM-DVA consists of only one mass coupled to the primary structure. The main difference between the traditional and proposed hybrid DVAs lies in the implementation of the control force. In the traditional DVA the control force is applied between the mass and the primary structure while in the new proposed DVA the control force acts between the masses. The performance of the proposed DM-DVA is evaluated experimentally by controlling the response of a cantilever beam under limited band white noise disturbance. The control approach is the feedforward algorithm. For the sake of comparison, the results are compared to the traditional hybrid SM-DVA.

2. THEORY

In this section, the dynamics of both SM and DM-DVAs are reviewed and compared. Without loss of generality, the primary structure to be controlled will be modelled as a single-degree-of-freedom (sdof) lumped parameter system. The primary structure can be characterized by its input or driving point impedance Z_p. Assuming a primary structure with viscous damping and a linear spring, the input impedance can be written as

$$Z_i = Z_p = C_p + \mathrm{i}(\omega M_p - K_p/\omega), \tag{1}$$

where M_p, C_p, and K_p are the mass, viscous damping, and stiffness constants of the primary structure, respectively; ω is the frequency of the disturbance; and i is the imaginary number.

2.1. HYBRID SINGLE-MASS DYNAMIC VIBRATION ABSORBER

The hybrid SM-DVA shown in Figure 1(b) consists of a mass, m_a, coupled to the primary structure through an elastic element with impedance $Z_E = c - \mathrm{i}k/\omega$, where k and c are the stiffness and damping of the elastic element. The active component is comprised of a self-balancing active force pair, which for simplicity will be referred to as the control

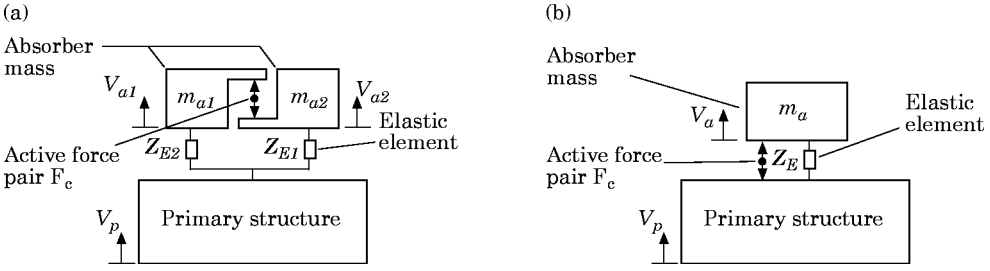

Figure 1. Schematic of (a) proposed dual-reaction mass and (b) traditional single-reaction mass dynamic vibration absorbers.

force F_C, located between the absorber mass and the primary structure. The motion of the new primary structure/hybrid SM-DVA system is written as

$$\begin{bmatrix} Z_p + Z_E & -Z_E \\ -Z_E & Z_a \end{bmatrix} \begin{Bmatrix} V_p \\ V_a \end{Bmatrix} = \begin{Bmatrix} F \\ 0 \end{Bmatrix} + \begin{Bmatrix} -F_C \\ F_C \end{Bmatrix}, \tag{2}$$

where $Z_a = Z_E + \mathrm{i}\omega m_a$ is the driving point impedance of the absorber alone, i.e. mounted to a rigid base instead of the primary system, F is the external force acting on the primary structure, and V_a is the velocity of the absorber's mass. The resonance of the SM-DVA corresponds to the minimum value of its driving impedance Z_a. For an undamped absorber, the natural frequency of the DVA is given as $\omega_a = \sqrt{k_a/m_a}$. The DVA's natural frequency is also referred to as the tuning frequency because the DVA is tuned by adjusting its natural frequency. For broadband frequency disturbances, the DVA's natural frequency is adjusted to match the resonance of the primary structure. For tonal disturbances, the DVA's natural frequency is designed to match the disturbance frequency [2].

Insight into the effects of the SM-DVA both as a passive and hybrid device on the primary response V_p is obtained by solving for the new input impedance of the combined system. For the SM-DVA used passively, i.e., $F_C = 0$, the input impedance seen by the force F is found from equation (2) as

$$Z_i = Z_p + \mathrm{i}\omega m_a Z_c / Z_a, \tag{3}$$

which shows that the input impedance has two components. The first term is the input impedance of the original primary structure Z_p, while the second term is the contribution due to the passive SM-DVA. This equation shows that the input impedance of the system becomes large at or near the tuning or natural frequency of the absorber, when Z_a becomes small. The large input impedance at this frequency is what yields the small response of the primary structure. In addition to raising the input impedance near the tuning frequency of the absorber, the SM-DVA causes the input impedance to become small at the two new resonance frequencies which are the minimums of equation (3).

It is clear that the passive SM-DVA is effective at or near its tuning frequency. Away from its tuning frequency, the effect of the SM-DVA on the primary system may be detrimental. In applications where the SM-DVA will be required to work effectively over a broad range of frequencies, one possible solution is the hybrid SM-DVA. In practice, the control force will be obtained by implementing one of the many algorithms such as velocity feedback, adaptive feedforward, neural networks, and so forth. Each one of these control approaches offers some unique advantages and drawbacks. The performance of the hybrid DVA will clearly be influenced to some degree by the selected control algorithm. However, all control approaches have as a common goal the reduction of the primary response, i.e., increasing the input impedance Z_i. Thus, in this work, the *ideal* control force is defined as the force required to drive the response of the primary structure to zero, thereby increasing the input impedance of the system to infinity. This definition of the control force allows the study to concentrate on the physics of the DVA without introducing particularities associated with the control approach.

The *ideal* control force to disturbance force ratio is obtained by setting $V_p = 0$ in equation (2) and solving for the force ratio as

$$F_c / F = Z_a / \mathrm{i}\omega m_a, \tag{4}$$

which shows that the *ideal* control force that leads to an infinite input impedance is a function of only the DVA's properties. This equation shows that the *ideal* control force is small near the resonance of the absorber where Z_a is minimum.

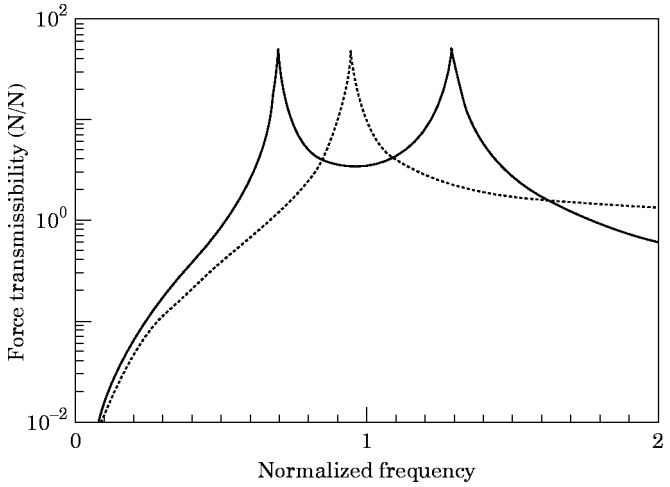

Figure 2. Magnitude of force transmissibility function of hybrid (——) DM-DVA and (·····) SM-DVA.

Further insight into the performance of the hybrid SM-DVA can also be gained by inspecting the hybrid SM-DVA's force transmissibility function. The force transmissibility function is defined here as the ratio of the total force applied by the hybrid SM-DVA into an infinite impedance to the control force applied to the hybrid SM-DVA. The total force applied by the SM-DVA, F_T, is due to the force transmitted by the elastic element, F_E, and the control force, F_C. Thus the force transmissibility function is easily found as

$$T_S = F_T/F_c = -\mathrm{i}\omega m_a/Z_a. \tag{5}$$

The magnitude of a typical force transmissibility function for the SM-DVA is shown in Figure 2 as a dotted line. For convenience, the frequency axis is normalized to the natural frequency of the primary system, $\omega_p = \sqrt{k_p/m_p}$. The behavior of the force transmissibility function can be efficiently investigated by plotting the force ratio $F_E/F_C = -Z_E/Z_a$. The magnitude and phase of this ratio for the SM-DVA is shown in Figure 3 as a dotted line. The characteristics of the force transmissibility function T_S can

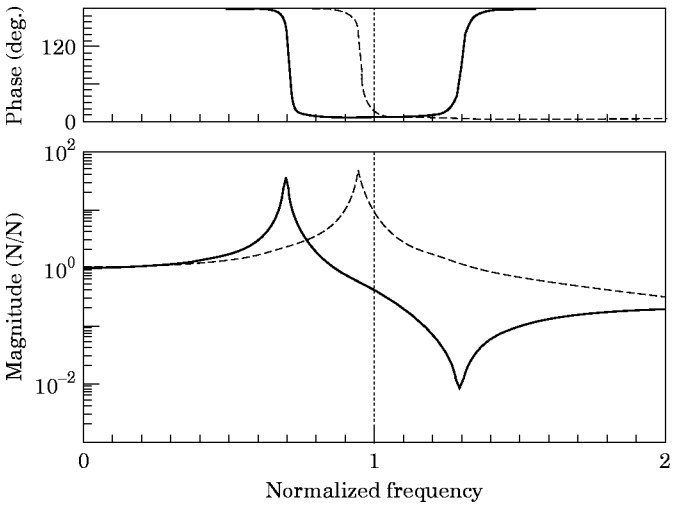

Figure 3. Magnitude and phase of force transfer function: ——, F_{E1}/F_{E2} of DM-DVA; ----, F_E/F_C of SM-DVA.

be categorized based on one of three frequency ranges of operation. At frequencies well below the resonant or tuning frequency, the two force components are nearly equal in magnitude and of opposite directions, i.e., $F_E \approx -F_C$, which leads the force transmissibility function to be significantly less than unity. Around the tuning frequency, the transmitted force is dominated by the elastic component which is significantly larger than the control force and in quadrature (i.e., $F_E \gg \mathrm{i}F_C$) due to the dynamic amplification of the DVA. In this frequency range, the total force on the input impedance is much larger than the control force applied to it and only limited by the damping in the DVA. This is the region where the SM-DVA is most effective and has the most control authority. Above the tuning frequency, the force transmissibility function starts decreasing, and approaches a value of unity at high frequencies since the elastic component vanishes due to the increase inertia of the DVA's mass, i.e., the SM-DVA neither amplifies nor attenuates the control force.

Comparison of equations 4 and 5 also reveals that the force transmissibility function is the negative inverse of the *ideal* control force required to drive the primary/hybrid DVA system's input impedance to infinity. For example, the larger the force transmissibility function the smaller the required *ideal* control force. Moreover, it is reasonable to assume that the hybrid SM-DVA with the highest force transmissibility function would require the least control effort to achieve a given primary response attenuation. Thus, based on this assumption, the force transmissibility function is proposed here as a *first metric* for evaluating the performance of hybrid SM-DVAs. The force transmissibility function has several characteristics which make it useful as a performance indicator: the force transmissibility function (1) does not depend on the characteristics of the primary structure, (2) is easily measured experimentally, and (3) is not dependent on the actual control algorithm which will be implemented.

It is important to remark that while the force transmissibility function is a good metric for comparing the hybrid SM-DVAs on the basis of the required control force, there are other factors to consider when selecting a hybrid SM-DVA for a specific application. For example, the stability of the control system is a critical issue if feedback control algorithms will be used. Also, causality of the control system is an important factor when using feedforward control approaches.

2.2. HYBRID DUAL-MASS DYNAMIC VIBRATION ABSORBER

The hybrid SM-DVA had one region of high force transmissibility near its resonance. In certain applications such as for a broadband disturbance, a DVA with high force transmissibility over a large frequency range may be required. The proposed hybrid DM-DVA overcomes this limitation.

The hybrid DM-DVA consists of two reaction masses, each coupled to the primary structure. The control force is applied between the masses as shown in Figure 1(a). The motion of the primary system coupled with the hybrid DM-DVA is described by

$$\begin{bmatrix} Z_p + Z_{E1} + Z_{E2} & -Z_{E1} & -Z_{E2} \\ -Z_{E1} & -Z_{a1} & 0 \\ -Z_{E2} & 0 & -Z_{a2} \end{bmatrix} \begin{Bmatrix} V_p \\ V_{a1} \\ V_{a2} \end{Bmatrix} = \begin{Bmatrix} F \\ 0 \\ 0 \end{Bmatrix} + \begin{Bmatrix} 0 \\ -F_C \\ F_C \end{Bmatrix}, \tag{6}$$

where $Z_{an} = Z_{En} + \mathrm{i}\omega m_{an}$ for $n = 1, 2$ is the driving point impedance of the nth reaction mass alone, and V_{a1} and V_{a2} are the velocities of the masses m_{a1} and m_{a2}, respectively. In equation (6), the coupling impedance between the absorber's masses is not included because it is detrimental to its performance [6].

The input impedance of the primary system with the passive DM-DVA is easily computed as

$$Z_i = Z_p + \mathrm{i}\omega m_{a1} Z_{E1}/Z_{a1} + \mathrm{i}\omega m_{a2} Z_{E2}/Z_{a2}, \tag{7}$$

which shows that the passive contribution of the DM-DVA to the input impedance of the system is simply the combination of the contribution of the two passive SM-DVAs.

As with the hybrid SM-DVA, the role of the control force is interpreted as actively increasing the input impedance of the primary structure. The *ideal* control force, which yields an infinite input impedance Z_i, is again obtained by setting the velocity of the primary structure $V_p = 0$ in equation (7). That is

$$F_C/F = Z_{a1} Z_{a2}/(Z_{E2} Z_{a1} - Z_{E1} Z_{a2}). \tag{8}$$

Once again the force transmissibility function of the hybrid DM-DVA T_D is defined as the net force generated on an infinite impedance by the absorber due to a unit control force. This leads to

$$T_D = F_T/F_c = -(Z_{E1} Z_{a2} - Z_{E2} Z_{a1})/Z_{a1} Z_{a2}. \tag{9}$$

As with the hybrid SM-DVA, comparing equations (8) and (9) shows that the negative inverse of the *ideal* control to disturbance force ratio is equal to the force transmissibility function of the hybrid DM-DVA.

The behavior of the force transmissibility function of the hybrid DM-DVA is now investigated and compared to the SM-DVA. To this end, the force transmissibility function T_D of the hybrid DM-DVA, which consists of the two elastic forces F_{E1} and F_{E2}, is shown in Figure 2 plotted as a solid line. In this figure, the hybrid DM-DVA has the same total reaction mass as the hybrid SM-DVA, $m_a = m_{a1} + m_{a2}$. The natural frequencies of the DM-DVA are set to 0·7 and 1·3 of the primary structure's natural frequency. The force transmissibility function of the hybrid DM-DVA has two peaks, one at each tuning frequency of the DM-DVA. At low frequencies, T_D diminishes as does T_S but not as steeply. Above the second resonance of the DM-DVA, T_D drops to a value lower than T_S and eventually vanishes. As with the SM-DVA, the total force applied by the DM-DVA has two components. A force is transmitted through each of the elastic coupling elements. Investigation of the relative magnitude and phase of these force components gives insight into the behavior of the DM-DVA. To this end, the ratio of the two elastic forces is given by

$$F_{E1}/F_{E2} = Z_{E1} Z_{a2}/Z_{E2} Z_{a1}, \tag{10}$$

which is shown in Figure 3 plotted as a solid line.

From Figures 2 and 3, at low frequencies the two forces are of nearly equal magnitude and opposite phase, so the force transmissibility is small. As the excitation frequency approaches the lower tuning frequency of the DM-DVA, the force applied by the lower resonant or first reaction mass becomes much larger than the other applied force. This result in a large force transmissibility function magnitude. Between the first and second tuning frequencies, neither of the masses are at a resonance condition, but the forces are in phase, and thus adding their effect to yield a high force transmissibility. At or near the second resonance frequency, the force applied by the second reaction mass is much larger than that from the first, again yielding a high transmissibility function magnitude. At frequencies well above the second resonance frequency of the DM-DVA, the applied forces are again of nearly equal magnitude and opposite phase. Thus, at high frequencies, the magnitude of the force transmissibility function of the hybrid DM-DVA approaches zero. Thus, the proposed DM-DVA configuration results in a high control authority over a

relatively wide frequency range. This range goes from frequencies lower than the first resonance to frequencies above the second resonance. This new DM-DVA actuator lends itself to applications where broadband control is desirable or where the excitation frequency varies significantly over a wide frequency range. Another advantage of this configuration is that it does not require the DVA's resonances to be tuned to the primary system resonance frequencies. This is important in feedback control approaches where the dynamics of the actuator have to be detuned from the primary system for stability reasons.

3. EXPERIMENTAL VALIDATION

In this section, the performance of the proposed DM-DVA is experimentally evaluated and compared to an equivalent SM-DVA system. The primary structure considered in the experiment was a steel beam, with a length of $L = 1{\cdot}15$ meters and cross-sectional dimensions of $38{\cdot}1 \times 25{\cdot}4$ mm. The beam had a total mass of 8·75 kg. It was mounted vertically with the base fixed to a granite table to simulate a fixed boundary condition while the other end of the beam is free. The beam was excited by a shaker, acting on the longer side of the cross section, positioned at 0·64 m from the fixed end.

To design the DVAs, the beam's natural frequencies had to be determined. For this simple structure, the natural frequencies can be predicted as $f_n = \lambda_n/2\pi L^2(EI/\rho A)^{1/2}$ with $\lambda_1 = 3{\cdot}516$, $\lambda_2 = 22{\cdot}03$, and $\lambda_3 = 61{\cdot}7$. Thus, the first three natural frequencies of the beam for the parameters $EI = 10\,405$ Nm^2 and $\rho A = 7{\cdot}6$ Ns^2/m^2 are $f_1 = 15{\cdot}64$, $f_2 = 98{\cdot}05$ and $f_3 = 256{\cdot}54$ Hz, respectively. An experiment was also conducted to determine the modal properties of the beam. The shaker was driven with white noise in the [0–200 Hz] frequency range to include the second mode of the beam. The excitation force was measured by a force transducer. The response of the beam was measured along its length every 10 cm using a moving accelerometer to identify the modes. The first and second resonances of the beam were found at 13 and 86 Hz, respectively, which agree well with analytically predicted values. Using the half power method, the damping ratios were estimated at 0·019 and 0·006 for the first and second mode, respectively. The modes of a fixed–free beam are well separated, so each mode behaves as a SDOF system. Thus, the second mode of the beam was targeted to be controlled using the hybrid DVAs.

The prototype actuator built for these experiments used a voice coil and rare-earth magnet assembly for actuation. Because the control force acts between the reaction masses in the hybrid DM-DVA, the magnet was fixed to one mass and the coil to the other mass, as shown in Figure 4. Both the masses were steel cylinders 44·5 mm in diameter and 20 mm tall. The first mass in Figure 4(a) had an elevated disk on one of its circular surfaces which was 1·5 mm thick. This disk was concentric with the axis of the mass. The purpose of the disk was to align the cylindrical voice coil with the axis of the mass. The mass also contained a linear bearing which was mounted axially. The second mass in Figure 4(b) had a hollow cavity in its center. A rare-earth magnet slug was mounted in this cavity and a circular steel cap was attached on top of the slug. The walls of the mass and the steel cap formed a path for the magnetic flux to flow across the voice coil gap. In addition, a steel alignment shaft extended from the top of the cap along the axis of the mass. By inserting the alignment shaft on the second mass into the linear bearing on the first mass, the voice coil was positioned so that it was set in the gap in the magnetic field path. A current passing through this coil induced a force pair which caused the masses to attract or repel each other.

The DM-DVA prototype was attached to the primary structure by means of a threaded attachment stud as shown in Figure 4(c). The masses were coupled to the primary structure through plate springs and a frame. The frame was designed to be much stiffer than the

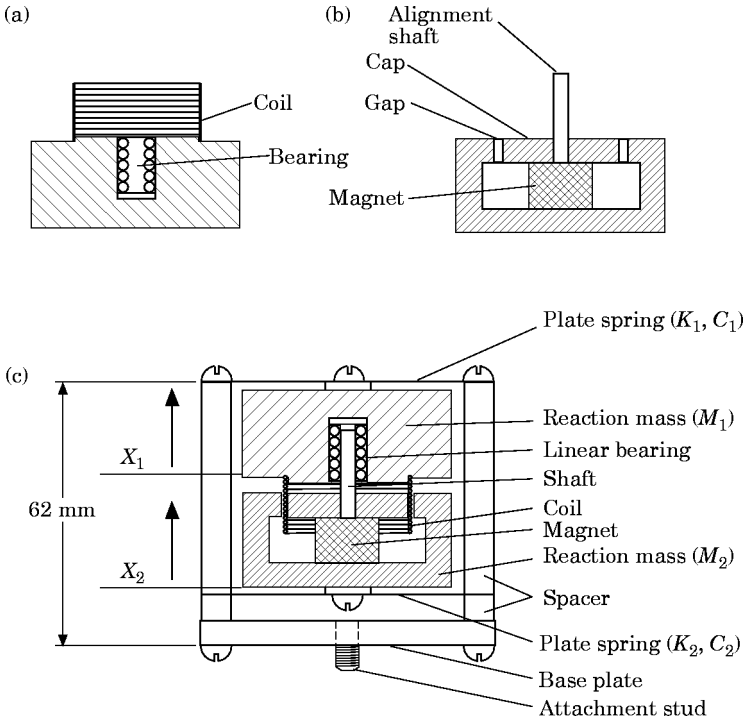

Figure 4. Prototype dual reaction mass absorber actuator: (a) elevated disk, (b) hollow cavity, (c) attachment schema.

springs. These springs were square brass plates connected to the frame at their four corners. Each mass was mounted axially to the center of the spring.The thickness and shape of the springs were adjusted to achieve a desired stiffness. The frame connected the plate springs to the primary structure. An aluminium plate ($50 \times 50 \times 6$ mm) was the base of the frame. Four spacers (6 mm diameter and 6 mm long) were placed at the corners of the base and supported by one of the spring/mass pairs. Four more spacers (6 mm diameter and 47 mm long) extended up from the corners of the spring. These spacers supported the second spring/mass pair. The bearing/shaft pair allowed relative motion between the masses while maintaining the axial alignment which kept the copper coil centered within the flux gap.

The prototype DVA could also be configured as a hybrid SM-DVA. To this end, one of the plate springs was replaced by a 6 mm thick aluminium plate which effectively locked the corresponding mass to the beam. Though locking one of the reaction-masses into place halved the SM-DVA's total reaction − mass as compared to the DM-DVA, a comparison of the performance between the two DVAs is valid. This is because the size of the mass of the SM-DVA affects only the amplitude of the response of the reaction mass and not the required control force. The main advantage of simply locking one of the masses is that the damping characteristics of the DVAs are equivalent. This is important because the damping has a significant effect on the active force required to achieve a certain level of vibration suppression.

The hybrid DM-DVA had two natural frequencies and two damping ratios in its operational frequency range, i.e., one for each spring/mass pair. Due to the compact construction of the hybrid DM-DVA, measuring the motion of the reaction masses was difficult. As shown in the theory, the force transmissibility function is an effective metric of the potential of a hybrid DVA as an actuator. Thus, the force transmissibility function

for both DVAs was experimentally measured. A high input impedance was obtained using a 20 kg steel block and the DM-DVA actuator was attached to the block through a force transducer. A white noise signal was applied to the hybrid DM-DVA and a force transducer measured the force applied by the DVA to the block. The experimental force transmissibility was measured using the voltage applied to the coil instead of the actual force generated. After locking one of the masses, the force transmissibility for the SM-DVA configuration was similarly measured. They are shown in Figure 5. The hybrid SM-DVA had a mass ratio of 3% as compared to the beam and thus the passive SM-DVA was tuned to 83 Hz which is optimal for this mass ratio [2, 7]. The DM-DVA's mass ratio is 5·4%. The DM-DVA resonances were adjusted by changing the spring constants to have one resonance above and one below the resonance of the beam, at 66 and 99 Hz, respectively. Unlike for the SM-DVA, these tuning frequencies were not optimized. The damping ratios of the hybrid SM and DM-DVAs estimated from the experimental transmissibility function were 3·6% for the SM-DVA and 2·6% and 4·5% for the DM-DVA. Notice that the damping ratio for the SM-DVA is close to the average of the damping ratios of the DM-DVA.

The control approach used was the broadband filtered-X LMS adaptive feedforward algorithm [8]. This algorithm requires a reference signal which is coherent with the disturbance. The reference signal is then filtered through a finite impulse response (FIR) control filter, i.e., compensator, to generate the control signal. The control filter's weights are then updated by the LMS algorithm which seeks to minimize the signal from the error sensor. A complete description of this control algorithm is beyond the scope of this paper and can be found in Vipperman *et al*. [8]. The FIR control filter had 255 coefficients. The sampling frequency of the controller was 800 Hz. The reference signal used by the controller was the same [0–200 Hz] band-limited white noise disturbance which was sent to the shaker. The disturbance sent to the shaker was delayed by 50 time steps to guarantee a causal system [9].

The vibration control test setup is shown in Figure 6. The shaker was again attached at 0·64 m from the base of the beam. The DVA was mounted at the free end of the beam while the error sensor, which was an accelerometer, was also mounted at the free end of the beam. The disturbance, control, and error signals were low-pass filtered with a cutoff

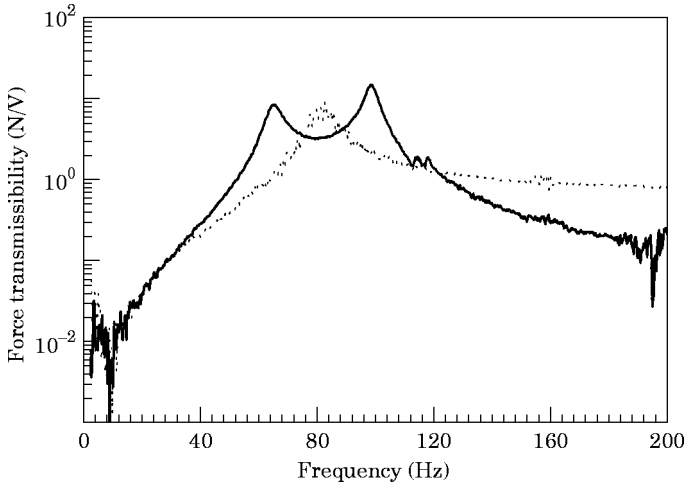

Figure 5. Experimentally measured magnitude of force transmissibility function of hybrid (——) DM-DVA and (. . . .) SM-DVA.

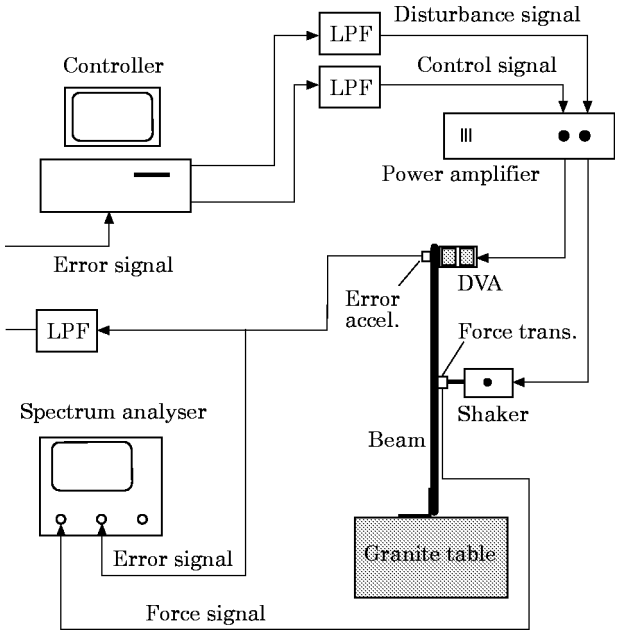

Figure 6. Schematic of active vibration control experimental setup.

frequency of 250 Hz. The error signal was amplified to use the full dynamic range of the controller.

3.1. EXPERIMENTAL RESULTS

The magnitude of the inertance of the free end of the original beam and the beam with the passive SM and DM-DVAs is presented in Figure 7. The passive SM-DVA significantly lowered the response of the beam at and near its tuned frequency of 83 Hz. As expected, two resonances are now present at 73 and 97 Hz. The SM-DVA had little effect on the first resonance of the beam. The root mean square (RMS) of the response was computed

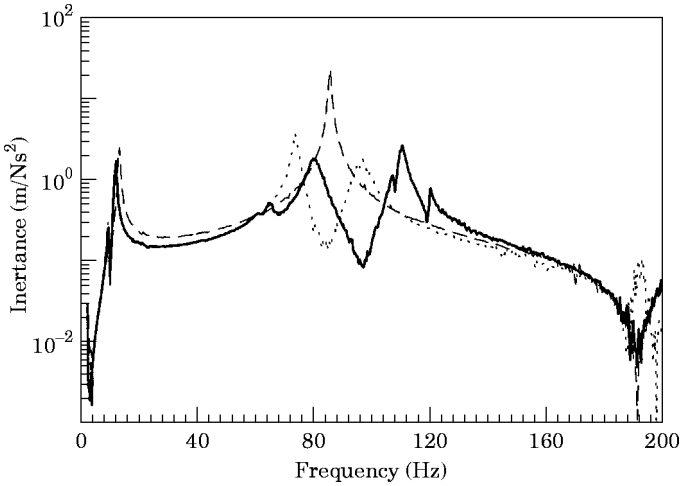

Figure 7. Inertance of the free end of the beam (- - - -) with no DVA, (. . .) with passive SM-DVA, and (——) with passive DM-DVA.

TABLE 1

RMS of error and control signals in the 20–200 *Hz frequency range. Reduction with respect to original beam system shown in parentheses*

System	RMS Error Signal (m/Ns^2)	RMS Control Signal (V/N)
Beam	55·3	–
Passive SM-DVA/Beam	16·0 (3·5)	–
Hybrid SM-DVA/Beam	4·8 (11·5)	4·9
Passive DM-DVA/Beam	14·8 (3·7)	–
Hybrid DM-DVA/Beam	4·5 (12·3)	2·7

by integrating the inertance over the frequency range 20–200 Hz to exclude the first mode of the beam which was not controlled. The results are summarized in Table 1. Over this frequency range, the passive SM-DVA lowered the RMS value of the error signal from 55·3 m/Ns^2 for the original beam to 16·0 m/Ns^2, reducing it by a factor of 3·5. On the other hand, the passive DM-DVA caused two notches in the beam response, at 67 and 97 Hz. It also yielded three resonances, at 65, 80 and 111 Hz. The passive DM-DVA also had little effect on the first mode of the beam. Over the same [20–200 Hz] frequency range, the passive DM-DVA lowered the RMS error signal from 55·3 to 14·8 m/Ns^2, reducing it by a factor of 3·7. Thus, as passive devices both DVAs performed efficiently.

The inertance of the free end of the beam with no DVAs and for the beam with the hybrid SM and DM-DVA systems is presented in Figure 8. The hybrid SM-DVA produced significant error signal reduction in the vicinity of the second resonance. The RMS value of the error signal in the 20–200 Hz frequency range was reduced from 55·3 m/Ns^2 of the original beam to 4·8 m/Ns^2, yielding a reduction factor of 11·5. In the same frequency range, the hybrid DM-DVA reduced the error signal level to 4·5 m/Ns^2, yielding a reduction factor of 12·3. The LMS algorithm did not seek to minimize the first mode of the beam with either hybrid DVA. At such low frequencies, the force transmissibility functions of both DVAs were sufficiently low that extremely high control forces would be required to achieve appreciable attenuation. At frequencies above 120 Hz, the SM-DVA

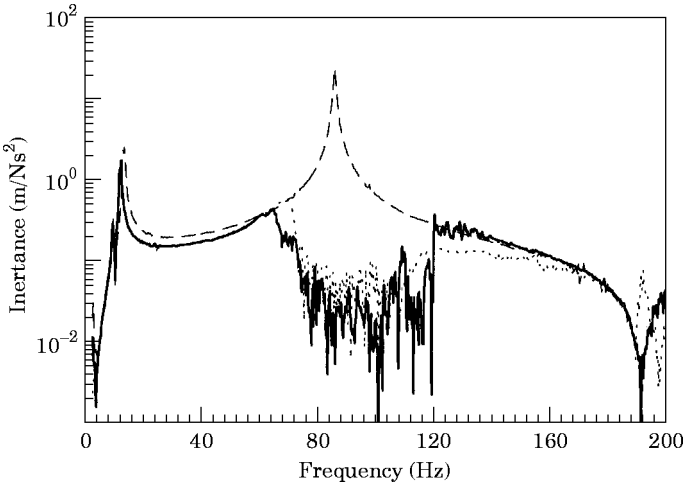

Figure 8. Inertance of the free end of the beam (— —) with no DVA, (. . .) with hybrid SM-DVA, and (——) with hybrid DM-DVA.

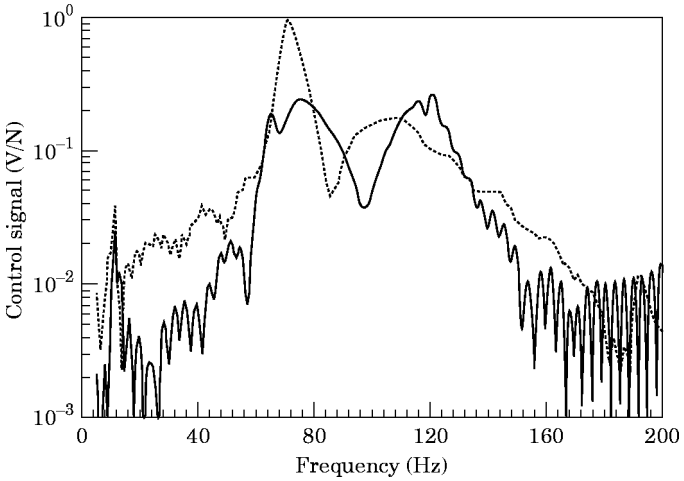

Figure 9. Spectrum of control signal for hybrid (. . . .) SM-DVA, and (——) DM-DVA.

was still able to achieve some attenuation. Beyond the resonance frequency of the SM-DVA, its force transmissibility function approaches unity which allows some control authority at high frequencies. On the other hand, the force transmissibility function of the hybrid DM-DVA approaches zero at high frequencies, giving it little control authority at these frequencies.

The magnitude of the control signal to disturbance force transfer function for the hybrid SM and DM-DVAs is shown in Figure 9. Across most of the frequency range, the hybrid SM-DVA required a higher control signal. The RMS values of the control signals in the 20–200 Hz frequency range were 4·9 and 2·7 Volts/N for the hybrid SM and DM-DVAs, respectively (see Table 1). These results indicate that the controller was able to cancel more of the disturbance using less control force with the hybrid DM-DVA as compared to the hybrid SM-DVA. These results clearly demonstrate the superior performance of the proposed hybrid DM-DVA.

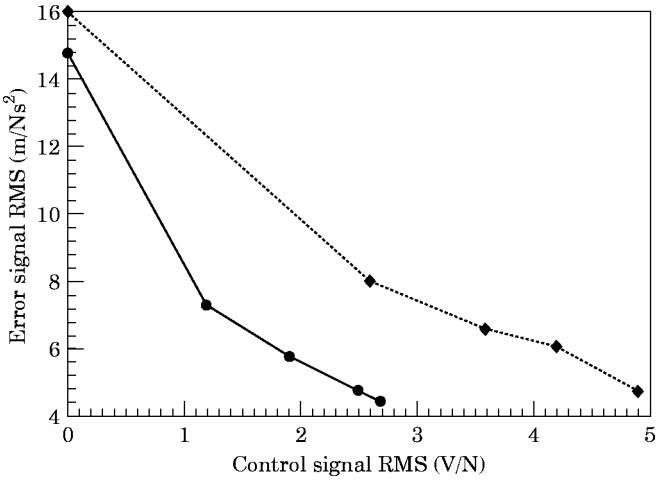

Figure 10. RMS of the error signal as a function of RMS of control signal for hybrid (. . . .) SM-DVA, and (——) DM-DVA.

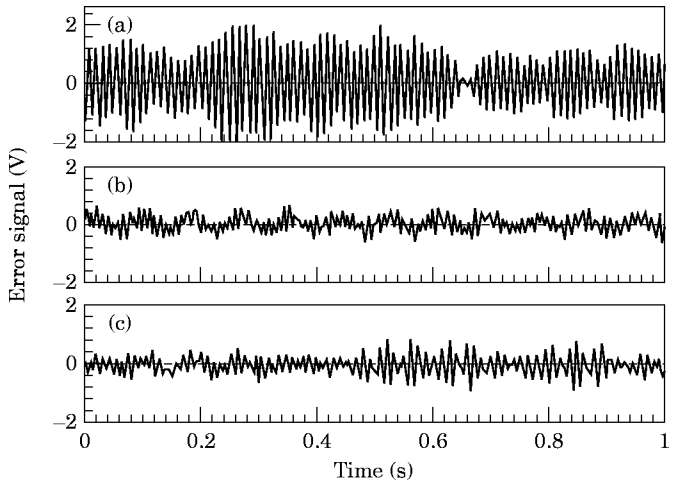

Figure 11. Time history of error signal for (a) original beam, (b) beam with passive SM-DVA, and (c) beam with passive DM-DVA.

The previous comparison between the hybrid SM and DM-DVAs was made after full controller convergence. To explore the control force/error signal relationship, the error and control signals were measured at various stages of controller convergence. The RMS value of the error signal is plotted as a function of the corresponding RMS value of the control signal in Figure 10. The RMS value of the error signal on the ordinate were those of the error signal levels achieved with the passive DVAs. This figure shows that regardless of the desired error signal level reduction, the control force required by the DM-DVA was always lower than for the SM-DVA. For example, the passive SM and DM-DVAs reduced the error signal RMS values to 16·0 and 14·8 m/Ns^2, respectively. To further reduce these levels by a factor of 2, the SM-DVA required a control force with an RMS value of 2·6 V/N. On the other hand, the DM-DVA required only 1·2 V/N (RMS), which was less than half the value required by the SM-DVA. Again it is shown that the hybrid DM-DVA allows the same vibration attenuation while requiring significantly less control force.

A time-domain comparison of the performance was also carried out. The reader should be aware that the measurements in the time domain were not normalized by the disturbance force. Figure 11(a) shows the time history of the error signal from the original beam. The RMS value of this error signal was 0·784 V. Figures 14(b) and 14(c) show the

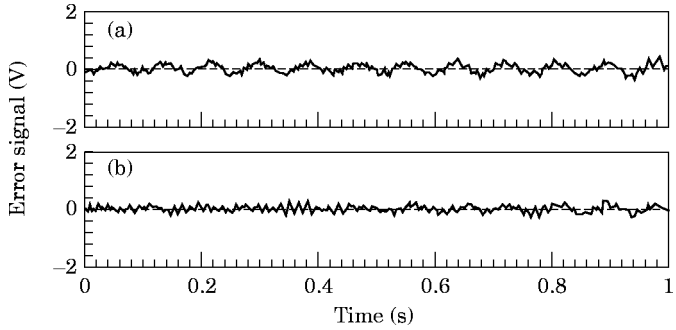

Figure 12. Time history of error signal for (a) beam with hybrid SM-DVA, and (b) beam with hybrid DM-DVA.

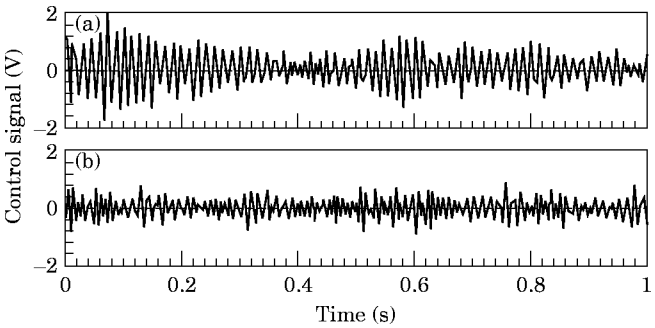

Figure 13. Time history of control signal of (a) hybrid SM-DVA and (b) hybrid DM-DVA.

error signal time histories from the beam/passive SM-DVA and beam/passive DM-DVA systems, respectively. The RMS value of these signals were 0·247 Volts and 0·187 Volts for the hybrid SM and DM-DVAs, respectively. Thus, the passive SM and DM-DVAs achieved reductions in the RMS value of the error signal level of 3·2 and 4·2, respectively.

Figures 12(a) and 12(b) present the error signals from the beam with the hybrid SM and DM-DVA, respectively. The RMS value of the signal in Figure 12(a) is 0·108 V which show a reduction by a factor of 7·3 as compared to the original system. The error signal from the beam with the hybrid DM-DVA has a RMS value of 0·106 V, which was a reduction by a factor of 7·4 as compared to the original beam. Figure 13(a) shows the control signal required by the hybrid SM-DVA. The RMS value of this signal was 0·549 V. Figure 13(b) shows the control signal required by the hybrid DM-DVA which had an RMS value of 0·288 V. The DM-DVA control signal was lower than that of the SM-DVA by a factor of 1·9. These results again show that the DM-DVA achieved higher error signal attenuation while requiring less control effort.

4. SUMMARY AND CONCLUSION

A new hybrid DVA configuration is presented which consisted of two reaction masses in parallel. Each of the masses was coupled to the primary structure through elastic elements with the active control force pair applied between the masses. The performance of the proposed hybrid dual-mass DVAs was evaluated experimentally and compared to the traditional SM-DVA. The filtered-X LMS feedforward algorithm to control the vibration of a fixed-free beam was selected as a test setup. The disturbance was band-limited white noise in the 0–200 Hz frequency range. The passive SM and DM-DVAs attenuated the response of the free end of the beam by factors of 3·5 and 3·7, respectively. The hybrid SM and DM-DVAs achieved reductions by factors of 11·5 and 12·3, respectively. The hybrid SM-DVA required a control effort of 4·9 V/N while the hybrid DM-DVA required 2·7 V/N, reducing it by a factor of 1·8. These results clearly demonstrate that the hybrid DM-DVA is superior to the hybrid SM-DVA, in particular, for broadband control applications. In addition, the force transmissibility function of hybrid DVAs is introduced and demonstrated to be an effective metric to determine the effectiveness of these devices.

REFERENCES

1. F. Hermann 1909 *German Patent* 525455. Device for Damping Vibrations of Bodies.
2. B. G. Korenev and L. M. Reznikov 1993 *Dynamic Vibration Absorbers*: *Theory and Technical Applications*. NY: John Wiley.

3. A. H. VON FLOTOW, A. BEARD and D. BAILEY 1994 *Proceedings of NOISE-CON* 94, *Ft. Lauderdale*, *Florida*, *May* 1–4 **1**, 437–454. Adaptive tuned vibration absorbers: tuning laws, tracking agility, sizing, and physical implementations.
4. J. Q. SUN, M. JOLLY and M. NORRIS 1995 *Transactions of the ASME* **117**, 234–242. Passive, adaptive and active tuned vibration absorbers—a survey.
5. R. A. BURDISSO and J. D. HEILMANN 1997 *Filed U.S. Patent* 08-825614. Active dual reaction mass actuator for vibration control.
6. J. D. HEILMANN 1996 *Master's Thesis*, *Virginia Polytechnic Institute and State University*. A dual reaction-mass dynamic vibration absorber for active vibration control.
7. J. C. SNOWDON 1968 *Vibration and Shock in Damped Mechanical Systems*. NY: John Wiley.
8. J. S. VIPPERMAN, R. BURDISSO and C. FULLER 1993 *Journal of Sound and Vibration* **166**, 283–299. Active control of broadband structural vibration using the LMS adaptive algorithm.
9. J. S. VIPPERMAN, R. BURDISSO and C. FULLER 1993 *Journal of the Acoustical Society of America* **94**, 234–242. Causality analysis of feedforward systems with broadband inputs.